

# Branching fractions and direct CP asymmetries of charmless decay modes at the Tevatron

M. Morello<sup>a</sup> on behalf of the CDF Collaboration

<sup>a</sup>Scuola Normale Superiore and INFN di Pisa - Ed. C, Polo Fibonacci, Largo B. Pontecorvo, 3 - 56127 Pisa, Italy

We present new CDF results on the branching fractions and time-integrated direct CP asymmetries for  $B^0$  and  $B_s^0$  decay modes into pairs of charmless charged hadrons (pion or kaon). The data set for this update amounts to  $1 \text{ fb}^{-1}$  of pp collisions at  $\sqrt{s} = 1.96 \text{ TeV}$ . We report the first observation of the  $B_s^0 \rightarrow K^+ K^-$  mode and a measurement of its branching fraction and direct CP asymmetry. We also observe for the first time two charmless decays of b-baryon:  $\Lambda_b^0 \rightarrow p \pi^-$  and  $\Lambda_b^0 \rightarrow p K^-$ .

## 1. INTRODUCTION

The decay modes of the B mesons into pairs of charmless pseudo-scalar mesons are effective probes of the quark-mixing (CKM) matrix and sensitive to potential new physics effects. The large production of B hadrons of all kinds at the Tevatron allows measuring such decays in new modes, which are important to supplement our understanding of B meson decays. The still unobserved  $B_s^0 \rightarrow K^+ K^-$  mode could be used to measure [1] and its CP asymmetry could be a powerful model-independent test of the source of the direct CP asymmetry in the B system [2]. This may provide useful information to solve the current discrepancy between the asymmetries observed in the neutral and charged mode [3].

The  $B_s^0 \rightarrow K^+ K^-$  and  $B^0 \rightarrow K^+ K^-$  modes proceed only through annihilation diagrams, which are currently poorly known and a source of significant uncertainty in many theoretical calculations [4,5]. A measurement of both modes would allow a determination of the strength of penguin-annihilation [6].

CDF II is a multipurpose magnetic spectrometer surrounded by calorimeters and muon detectors [7]. A silicon micro-strip detector (SVX II) and a cylindrical drift chamber (COT) immersed in a 1.4 T solenoidal magnetic field reconstruct charged particles in the pseudo-rapidity range

$|\eta| \leq 1.0$ . The SVX II consists of five concentric layers of double-sided silicon detectors with radii between 2.5 and 10.6 cm, each providing a measurement with 15  $\mu\text{m}$  resolution in the direction and 70  $\mu\text{m}$  in z direction. The COT has 96 measurement layers, between 40 and 137 cm in radius, organized into alternating axial and 2 stereo super-layers. The transverse momentum resolution is  $\sigma_{p_T} = p_T \cdot 0.15\% p_T / (\text{GeV}/c)$  and the observed mass-widths are about  $14 \text{ MeV}/c^2$  for  $J/\psi \rightarrow K^+ K^-$  decays, about  $9 \text{ MeV}/c^2$  for  $D^0 \rightarrow K^+ K^-$  decays. The specific energy loss by ionization ( $dE/dx$ ) of charged particles in the COT can be measured from the amount of charge collected by each wire.

Throughout this paper, C-conjugate modes are implied and branching fractions indicate CP-averages unless otherwise stated.

## 2. DATA SAMPLE

We analysed a  $\sqrt{s} = 1.96 \text{ TeV}$  sample of pairs of oppositely-charged particles with  $p_T > 2 \text{ GeV}/c$  and  $p_T(1) + p_T(2) > 5.5 \text{ GeV}/c$ , used to form  $B_{(s)}^0$  meson candidates. The trigger required also a transverse opening-angle  $20^\circ < \Delta\phi < 135^\circ$  between the two tracks, to reject background from particle pairs within the same jet and from back-to-back jets. In addition, both charged particles were required to originate from a displaced vertex with a large impact parameter  $d_0 > 100 \text{ nm}$

$< d_0 < 1 \text{ mm}$ ), while the  $B_{(s)}^0$  meson candidate was required to be produced in the primary pp interaction ( $d_0(B) < 140 \text{ m}$ ) and to have travelled a transverse distance  $L_{xy}(B) > 200 \text{ m}$ .

In the online analysis, an unbiased optimization procedure determined a tightened selection on track-pairs fit to a common decay-vertex. We chose the selection cuts minimizing directly the expected uncertainty (through several pseudo-experiments) of the physics observables to be measured. We decided to use just two different sets of cuts, respectively optimized to measure  $A_{CP}(B^0 \rightarrow K^+ K^-)$  and  $B(B_s^0 \rightarrow K^+ K^-)$ , since those two measurements are the main focus of the analysis. For the latter the sensitivity for discovery and limit setting [8] was optimized rather than the statistical uncertainty on the particular parameter, since the mode had not yet been observed. It was verified that the former set of cuts is also adequate to measure other decay rates of the larger yield modes ( $B^0 \rightarrow \pi^+ \pi^-$ ,  $B_s^0 \rightarrow K^+ K^-$ ), while the latter, tighter set of cuts, is well suited to measure the decay rates and CP asymmetries related to rare modes ( $B_s^0 \rightarrow \pi^+ \pi^-$ ,  $B^0 \rightarrow K^+ K^-$ ,  $B_b^0 \rightarrow p \bar{p}$ ,  $B_b^0 \rightarrow p \bar{K}$ ).

In addition to tightening the trigger cuts, in the online analysis the discriminating power of the  $B_{(s)}^0$  meson 'isolation' and of the information provided by the 3D reconstruction capability of CDF tracking were used, allowing a great improvement in the signal purity. Isolation is defined as  $I(B) = p_T(B) / [p_T(B) + \sum_i p_T(i)]$ , in which the sum runs over every other track within a cone of radius one in the  $\eta$  space around the  $B_{(s)}^0$  meson flight-direction. By requiring  $I(B) > 0.5$  we reduced the background by a factor four while keeping almost 80% of signal. The 3D silicon tracking allowed to resolve multiple vertices along the beam direction and to reject fake tracks reducing the background by a factor of two, with small inefficiency on signal. The resulting  $m$  and  $m_{12}$  distributions (Fig. 3) show a clean signal of  $B_{(s)}^0 \rightarrow h^+ h^-$  decays. In spite of a good  $m$  mass resolution ( $\approx 22 \text{ MeV}/c^2$ ), the various  $B_{(s)}^0 \rightarrow h^+ h^-$  modes overlap into an unresolved  $m$  mass peak.

### 3. FIT OF COMPOSITION

The resolution in invariant mass and in particle identification is not sufficient for separating the individual decay modes on an event-by-event basis therefore we performed an unbinned maximum likelihood fit, combining kinematic and particle identification information, to statistically determine the contribution of each mode and the CP asymmetries. For the kinematic portion, we used three loosely correlated observables to summarize the information carried by all possible values of invariant mass of the B candidate, resulting from different mass assignments to the two outgoing particles [9]. They are: (a) the mass  $M_{12}$  calculated with the charged pion mass assignment to both particles; (b) the signed momentum imbalance  $\Delta = (1 - p_1/p_2)q_1$ , where  $p_1$  ( $p_2$ ) is the lower (higher) of the particle momenta, and  $q_1$  is the sign of the charge of the particle of momentum  $p_1$ ; (c) the scalar sum of the particle momenta  $p_{\text{tot}} = p_1 + p_2$ . Using these three variables, the mass of any particular mode  $M_{12}$  can be written as:

$$M_{12}^2 = M^2 - \frac{2m^2 + (m_1^2 + m_2^2)}{q} + \frac{2(p_1^2 + m^2)}{q} - \frac{p_2^2 + m^2}{q} + \frac{2(p_1^2 + m_1^2)}{q} - \frac{p_2^2 + m_2^2}{q}; \quad (1)$$

$$p_1 = \frac{1}{2} \frac{p_j}{p_{\text{tot}}}; \quad p_2 = \frac{1}{2} \frac{p_{\text{tot}}}{p_j}; \quad (2)$$

where  $m_1$  ( $m_2$ ) is the mass of the lower (higher) momentum particle. For simplicity the Eq. (1) is written as a function of  $p_1$  and  $p_2$  instead of  $m$  and  $p_{\text{tot}}$  but in the likelihood it is used as a function of  $m$  and  $p_{\text{tot}}$ . Particle identification (PID) information is summarized by a single observable for each track defined as  $\mathcal{P} = \frac{dE/dx}{dE/dx(K)} \cdot \frac{dE/dx(\pi)}{dE/dx(\pi)}$ . With the chosen observables, the likelihood contribution of the  $i^{\text{th}}$  event is written as:

$$L_i = (1 - b) \prod_j f_j L_j^{\text{kin}} L_j^{\text{PID}} + b f_A L_A^{\text{kin}} L_A^{\text{PID}} + (1 - f_A) L_E^{\text{kin}} L_E^{\text{PID}} \quad (3)$$

where:

$$L_j^{\text{kin}} = R(M_j - M_j(\mathbf{p}_{\text{tot}}); \mathbf{p}_{\text{tot}}) P_j(\mathbf{p}_{\text{tot}}); \quad (4)$$

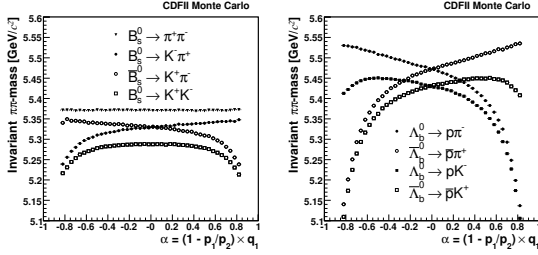


Figure 1. Average  $M$  vs  $\alpha$  for simulated samples of  $B_s^0$  (left) and  $B_b^0$  (right) candidates, where self-tagging final states ( $K^+$  and  $K^+$ ,  $ph$  and  $ph^+$ ) are treated separately. The corresponding plots for the  $B^0$  are similar to  $B_s^0$  but shifted for the mass difference.

$$L_A^{kin} = A(M_j; m_0) P_A(\alpha; p_{tot}); \quad (5)$$

$$L_E^{kin} = e^{c_1 M} P_E(\alpha; p_{tot}); \quad (6)$$

$$L_{j(E;A)}^{PID} = F_{j(E;A)}(1; 2; \alpha; p_{tot}); \quad (7)$$

The index  $A(E)'$  labels the physical (combinatorial) background-related quantities, the index  $j$  runs over the twelve distinguishable  $B_{(s)}^0 \rightarrow h^+ h^0$  and  $B_b^0 \rightarrow ph$  modes (Fig. 1), and  $f_j$  are their fractions, to be determined by the fit together with the total background fraction  $b$  and with the fraction of the physical (combinatorial) background  $f_{A(E)}$ . The conditional probability density  $R(M_j; \alpha; p_{tot})$  is the mass resolution function of each mode  $j$  when the correct mass is assigned to both tracks. In fact the average mass  $M_j(\alpha; p_{tot})$  is the value of  $M$  obtained from Eq. (1) by setting the appropriate particle masses for each decay mode  $j$  and making a simple variable change we obtain  $R(M_j; \alpha; p_{tot}) = R(M_j; M_{B^0(B_s^0; B_b^0)}; \alpha; p_{tot})$  where  $M_j$  is the invariant mass computed with the correct mass assignment to both particles for each mode  $j$ .  $R$  was parameterized using the detailed detector simulation. To keep into account non-Gaussian tails due to the emission of photons in the final state, we included in the simulation the

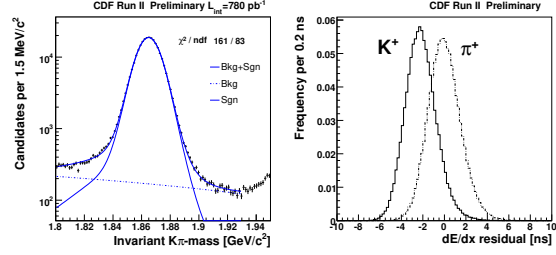


Figure 2. Tagged  $D^0 \rightarrow K^+$  decays from  $D^+ \rightarrow D^0 + [K^+]^+$ . Check of the mass line shape template performing a 1-dimensional binned fit where the signal mass line shape is completely fixed from the model (left). Distribution of  $dE/dx$  (mean COT pulse-width) around the average pion response, for calibration samples of kaons and pions (right).

soft photon emission in agreement with recent QED calculations [10]. We checked the quality of the mass resolution model using about 500K  $D^0 \rightarrow K^+$  decays (Fig. 2, left). We fitted the mass line-shape of the  $D^0 \rightarrow K^+$  peak fixing the signal shape from the model and allowing to vary only the background function. We obtained a good agreement between data and simulation. In Eq. (4), we used the nominal  $B^0$ ,  $B_s^0$  and  $B_b^0$  masses measured by CDF [11] to cancel the common systematic uncertainty. The background mass distribution is determined in the fit by varying the parameters  $c_1$ ,  $c_2$  and  $m_0$  in Eq. (5,6).  $c_2$  and  $m_0$  are the parameters of an 'Argus' function [13] smeared with a Gaussian distribution centered in zero with a width equal to the mass resolution. The  $P_j(\alpha; p_{tot})$  is the joint probability distribution of  $(\alpha; p_{tot})$  and is parameterized for each mode  $j$  by a product of polynomial and exponential functions fitted to Monte Carlo samples produced by a detailed detector simulation. The background function  $P_{A(E)}$  is obtained from the mass sidebands of data.

A sample of 1.5M  $D^+ \rightarrow D^0 + [K^+]^+$  decays, where the  $D^0$  decay products are identified by the charge of the  $D^+$  pion, was used

to calibrate the  $dE=dx$  response over the tracking volume and time, and to determine the  $F$  functions in (7). In a  $> 95\%$  pure  $D^0$  sample, we obtained 1:4 separation between kaons and pions (Fig. 2, right), corresponding to an uncertainty on the measured fraction of each class of particles that is just 60% worse than the uncertainty attainable with ideal separation. The background term in (7) is similar to the signal terms, but allows for independent pion, kaon, proton, and electron components, which are free to vary independently. Muons are indistinguishable from pions with the available  $dE=dx$  resolution.

#### 4. FIT RESULTS AND SYSTEMATICS

We performed two separate fits: the first one using the cuts optimized to measure the direct  $A_{CP}(B^0 \rightarrow K^+)$  and the second one to measure  $B(B_s^0 \rightarrow K^+)$ . Significant signals are seen for  $B^0 \rightarrow \pi^+$ ,  $B^0 \rightarrow K^+$ , and  $B_s^0 \rightarrow K^+K^-$  mode, previously observed by CDF [12], three new rare modes were observed for the first time:  $B_s^0 \rightarrow K^+$ ,  $B_b^0 \rightarrow p$  and  $B_b^0 \rightarrow pK^+$  while no evidence was obtained for  $B_s^0 \rightarrow \pi^+$  and  $B^0 \rightarrow K^+K^-$  mode.

To convert the yields returned from the fit into relative branching fractions, we applied corrections for efficiencies of trigger and online selection requirements for different decay modes. The relative efficiency corrections between modes do not exceed 20%. Most corrections were determined from the detailed detector simulation, with some exceptions which are measured using data. A momentum-averaged relative isolation efficiency between  $B_s^0$  and  $B^0$  of  $1.07 \pm 0.11$  was determined from fully-reconstructed samples of  $B_s^0 \rightarrow J/\psi$ ,  $B_s^0 \rightarrow D_s^+ \pi^-$ ,  $B^0 \rightarrow J/\psi K^0$ , and  $B^0 \rightarrow D^+ \pi^-$ . The lower specific ionization of kaons with respect to pions in the drift chamber is responsible for a  $\sim 5\%$  lower efficiency to reconstruct a kaon. This effect was measured in a sample of  $D^+ \rightarrow K^+ \pi^+$  decays triggered on two tracks, using the unbiased third track. The only correction needed by the direct CP asymmetries  $A_{CP}(B^0 \rightarrow K^+)$  and  $A_{CP}(B_s^0 \rightarrow K^+)$  was a  $0.6\%$  shift due to the different probability for  $K^+$  and  $K^-$  to interact with the tracker

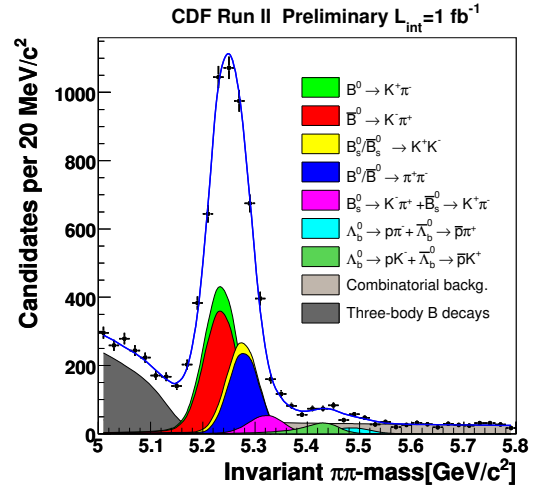


Figure 3. Invariant mass distribution of  $B^0 \rightarrow h^+ h^0$  candidates passing all selection requirements optimized to measure  $B(B_s^0 \rightarrow K^+)$ , using a pion mass assumption for both decay products. Cumulative projections of the likelihood fit for each mode are overlaid.

material. The measurement of this correction has been done using a sample of 1M of prompt  $D^0 \rightarrow K^+ \pi^-$  decays reconstructed and selected using the same criteria of  $B_{(s)}^0 \rightarrow h^+ h^0$  decays. Assuming the Standard Model expectation  $A_{CP}(D^0 \rightarrow K^+) = 0$ , the difference between the number of reconstructed  $D^0 \rightarrow K^+ \pi^-$  and  $\bar{D}^0 \rightarrow K^+ \pi^-$  provides a measurement of the detector-induced asymmetry between  $K^+$  and  $K^-$  final states. Since we used the same technique developed for the  $B_{(s)}^0 \rightarrow h^+ h^0$  decays, this measurement provides also a robust check on all possible charge asymmetry biases of the detector and  $dE=dx$  parameterizations.

The  $B_s^0 \rightarrow K^+ K^-$  and  $B_s^0 \rightarrow \pi^+ \pi^-$  modes required a special treatment, since they contain a superposition of the flavor eigenstates of the  $B_s^0$ . Their time evolution might differ from the one of the flavor-specific modes if the width difference  $\Gamma_{12}$  between the  $B_s^0$  mass eigenstates is significant. The current result was derived under the

assumption that both modes are dominated by the short-lived  $B_s^0$  component, that  $\tau_{s^*} = \tau_d$ , and  $\tau_{s^*} = \tau_s = 0.12 \pm 0.06$  [14,15]. The latter uncertainty is included in estimating the overall systematic uncertainty.

The dominant contributions to the systematic uncertainty are: the statistical uncertainty on isolation efficiency ( $B_s^0$  modes), the uncertainty on the  $dE/dx$  calibration and parameterization and the uncertainty of the combinatorial background model. The first one is the larger systematic of all measurements with the meson  $B_s^0$  in the initial state (except for  $A_{CP}(B_s^0 \rightarrow K^+)$ ). This uncertainty is preliminary and conservative, a significant improvement is expected for the final results. The second one, due to  $dE/dx$ , is a large systematic of all measurements, although the parameterization of the  $dE/dx$  is very accurate. The effect of composition is very sensitive to the PID information. The third one is due to the statistical uncertainty of the possible combinatorial background models and it is a dominant systematic for the observables of the rare modes. Smaller systematic uncertainties are assigned for: trigger efficiencies; physical background shape and kinematics;  $B$  meson masses, lifetimes.

## 5. RESULTS

The relative branching fractions are listed in Tab. (1), where  $f_d$  and  $f_s$  indicate the production fractions respectively of  $B^0$  and  $B_s^0$  from fragmentation of a  $b$  quark in  $pp$  collisions. An upper limit is also quoted for modes in which no significant signal is observed [16]. We also list absolute results obtained by normalizing our data to the world-average of  $B(B^0 \rightarrow K^+)$  [3].

We report the first observation of three new rare charmless decays  $B_s^0 \rightarrow K^+ \pi^-$ ,  $B_s^0 \rightarrow p \pi^-$  and  $B_s^0 \rightarrow p K^-$  with a significance respectively of 8.2, 6 and 11.5. The significance includes both statistical and systematic uncertainty. The statistical uncertainty to evaluate the significance was estimated using several pseudo-experiments with no contributions from rare signals.

The rate of the newly observed mode  $B(B_s^0 \rightarrow K^+) = (5.0 \pm 0.75 \pm 1.0) \cdot 10^6$  is in agreement with the latest theoretical expectation [17] which

is lower than the previous predictions [4,18]. We measured for the first time in the  $B_s$ -meson system its direct CP asymmetry  $A_{CP}(B_s^0 \rightarrow K^+) = 0.39 \pm 0.15 \pm 0.08$ . This value favors a large CP violation in the  $B_s^0$  mesons, on the other hand it is also compatible with 0. In [2] it is suggested a robust test of the Standard Model vs New Physics by comparison of the direct CP asymmetries in the  $B_s^0 \rightarrow K^+$  and  $B^0 \rightarrow K^+$  decays. Using HFAG input [3] we measured  $\frac{B(B_s^0 \rightarrow K^+) \cdot A_{CP}(B_s^0 \rightarrow K^+)}{B(B^0 \rightarrow K^+) \cdot A_{CP}(B^0 \rightarrow K^+)} = 0.84 \pm 0.42 \pm 0.15$  (where  $\Gamma$  is the decay width) in agreement with the Standard Model expectation ( $= 1$ ).

Assuming that the relationship above is  $= 1$  and using as input the  $B(B_s^0 \rightarrow K^+)$  measured here, the world average for  $A_{CP}(B^0 \rightarrow K^+)$  and the  $B(B^0 \rightarrow K^+)$  [3] we can estimate the expected value for  $A_{CP}(B_s^0 \rightarrow K^+) = 0.37$  in agreement with our measurement.

The rate of the mode  $B(B_s^0 \rightarrow K^+ K^-) = (24.4 \pm 1.4 \pm 4.6) \cdot 10^6$  is in agreement with the latest theoretical expectation [19,20] and with the previous CDF measurement [12]. An improved systematic uncertainty is expected for the final analysis of the same sample.

The results for the  $B^0$  are in agreement with world average values [3]. The measurement  $A_{CP}(B^0 \rightarrow K^+) = 0.086 \pm 0.023 \pm 0.009$  is the world's second best measurement and the significance of the new world average  $A_{CP}^{ave}(B^0 \rightarrow K^+) = 0.095 \pm 0.013$  moved from 6 to 7.

We updated the upper limits and we quoted also the absolute branching fractions of the currently unobserved annihilation-type modes:  $B^0 \rightarrow K^+ K^-$  and  $B_s^0 \rightarrow \pi^+ \pi^-$ . The rate  $B(B^0 \rightarrow K^+ K^-) = (0.39 \pm 0.16 \pm 0.12) \cdot 10^6$  has the same uncertainty of the current measurements [3] while the  $B_s^0 \rightarrow \pi^+ \pi^-$  upper limit (already the world's best one [12]) was improved by a factor 1.3, approaching the expectations from recent calculations [5,21].

We also report the first observation of two new baryon charmless modes  $B_b^0 \rightarrow p \pi^-$  and  $B_b^0 \rightarrow p K^-$ . We measured  $B(B_b^0 \rightarrow p \pi^-) = B(B_b^0 \rightarrow p K^-) = 0.66 \pm 0.14 \pm 0.08$  in agreement with the expectations from [22].

Table 1

Results on data sample optimized to measure  $A_{CP}(B^0 \rightarrow K^+)$  (top) and  $B(B_s^0 \rightarrow K^+)$  (bottom). Absolute branching fractions are normalized to the world average values  $B(B^0 \rightarrow K^+) = (19.7 \pm 0.6) \cdot 10^{-6}$  and  $f_s = (10.4 \pm 1.4)\%$  and  $f_d = (39.3 \pm 1.0)\%$  [3]. The first quoted uncertainty is statistical, the second is systematic.

mode	$N_s$		Quantity	Measurement			$B(10^{-6})$			
$B^0 \rightarrow K^+$	4045	84	$\frac{B(B^0 \rightarrow K^+)}{B(B^0 \rightarrow K^+) + B(B^0 \rightarrow K^+)}$	-0.086	0.023	0.009				
$B^0 \rightarrow K^+$	1121	63	$\frac{B(B^0 \rightarrow K^+)}{B(B^0 \rightarrow K^+)}$	0.259	0.017	0.016	5.10	0.33	0.36	
$B_s^0 \rightarrow K^+ K$	1307	64	$\frac{f_s B(B_s^0 \rightarrow K^+ K)}{f_d B(B^0 \rightarrow K^+)}$	0.324	0.019	0.041	24.4	1.4	4.6	
$B_s^0 \rightarrow K^+$	230	34	16	$\frac{f_s B(B_s^0 \rightarrow K^+)}{f_d B(B^0 \rightarrow K^+)}$	0.066	0.010	0.010	5.0	0.75	1.0
				$\frac{B(B_s^0 \rightarrow K^+) B(B_s^0 \rightarrow K^+)}{B(B_s^0 \rightarrow K^+) + B(B_s^0 \rightarrow K^+)}$	0.39	0.15	0.08			
				$\frac{f_d B(B_s^0 \rightarrow K^+)}{f_s B(B^0 \rightarrow K^+)}$	-3.21	1.60	0.39			
$B_s^0 \rightarrow K^+$	26	16	14	$\frac{f_s B(B_s^0 \rightarrow K^+)}{f_d B(B^0 \rightarrow K^+)}$	0.007	0.004	0.005	0.53	0.31	0.40
								(< 1.36 @ 90% CL)		
$B^0 \rightarrow K^+ K$	61	25	35	$\frac{B(B^0 \rightarrow K^+ K)}{B(B^0 \rightarrow K^+)}$	0.020	0.008	0.006	0.39	0.16	0.12
								(< 0.7 @ 90% CL)		
$B_b^0 \rightarrow pK$	156	20	11	$\frac{B(B_b^0 \rightarrow pK)}{B(B_b^0 \rightarrow pK)}$	0.66	0.14	0.08			
$B_b^0 \rightarrow p$	110	18	16							

## REFERENCES

- M. Gronau and J. L. Rosner, Phys. Lett. B 482, 71 (2000).
- H. J. Lipkin, Phys. Lett. B 621, 126 (2005).
- E. Barberio et al. [Heavy Flavor Averaging Group (HFAG)], arXiv:hep-ex/0603003.
- M. Beneke and M. Neubert, Nucl. Phys. B 675, 333 (2003).
- Y. D. H. Yang et al., arXiv:hep-ph/0507326
- A. J. Buras et al., Nucl. Phys. B 697, 133 (2004).
- D. A. Costa et al. (CDF Collaboration), Phys. Rev. D 71, 032001 (2005).
- G. Punzi, eConf C 030908, MODT002 (2003); arXiv:physics/0308063.
- For a discussion of the bias in multi-component fits related to the use of multiple variables see G. Punzi, eConf C 030908, WELT002 (2003); arXiv:physics/0401045.
- E. Baracchini and G. Isidori, Phys. Lett. B 633, 309 (2006).
- D. A. Costa et al. (CDF Collaboration), Phys. Rev. Lett. 96, 202001 (2006).
- A. Abulencia et al. (CDF Collaboration), Phys. Rev. Lett. 97, 211802 (2006).
- $A(x; j_2; m_0) = \text{Norm} \left[ x e^{-c_2 \left(\frac{x}{m_0}\right)^2} \frac{1}{1 + \left(\frac{x}{m_0}\right)^2} \right]$  if  $x < m_0$ ,  $A(x; j_2; m_0) = 0$  if  $x > m_0$ .
- M. Beneke et al., Phys. Lett. B 459, 631 (1999).
- A. Lenz, arXiv:hep-ph/0412007.
- We use frequentist limits based on Gaussian distribution of  $t$  pulls (with systematics added in quadrature), and LR-ordering; see G. J. Feldman and R. D. Cousins, Phys. Rev. D 57, 3873 (1998).
- A. R. Williamson, J. Zupan, Phys. Rev. D 74, 014003 (2006).
- Xian-Qiao Yu et al., Phys. Rev. D 71, 074026, (2005)
- S. Descotes-Genon et al., Phys. Rev. Lett. 97 061801 (2006).
- S. Baek et al., arXiv:hep-ph/0610109.
- Y. Li et al., Phys. Rev. D 70, 034009 (2004).
- R. Mohanta et al. Phys. Rev. D 63, 074001 (2001).